

Original Research

Identification and Monitoring of Surface Elements in Open-Pit Coal Mine Area Based on Multi-Source Remote Sensing Images

Wenyue Hai^{1,2,3}, Nan Xia^{1,2,3*}, Jimei Song^{1,2,3}, Mengying Tang^{1,2,3}

¹College of Geographical and Remote Sensing Science, Xinjiang University (China),
777 Huarui Street, Shuimogou District, Urumqi, Xinjiang, China

²Xinjiang Key Laboratory of Oasis Ecology, Xinjiang University (China),
777 Huarui Street, Shuimogou District, Urumqi, Xinjiang, China

³Key Laboratory of Smart City and Environment Modelling of Higher Education Institute, Xinjiang University (China),
777 Huarui Street, Shuimogou District, Urumqi, Xinjiang, China

Received: 31 January 2022

Accepted: 6 April 2022

Abstract

Coal mining has brought a series of environmental problems. Local government departments have issued relevant governance policies, but the premise of scientific prevention and control is to correctly grasp the actual distribution of various ground objects in the mining area. Using classification methods to extract ground object information based on remote sensing images can effectively realize mining area monitoring and provide reference for land and space planning and environmental protection in the mining area. Therefore, it is very important to select the appropriate scale and method to identify the ground object information of remote sensing image. In this paper, Landsat 8 images of the Wucaiwan mining area and GF-2 images of the Tebian coal mine were taken as the research objects, and unsupervised classification, supervised classification and object-oriented classification were used to identify and monitor the mining area's surface. The results showed that: (1) the classification effect of the Mahalanobis distance method was the best in terms of comprehensive operation process and classification accuracy. This method had high classification accuracy for GF-2 and Landsat 8 images. When classifying GF-2 images, the kappa coefficient reached 0.90, and the overall classification accuracy was 94.27%. When classifying Landsat 8 images, the kappa coefficient reached 0.85, and the overall classification accuracy was 90.02%. (2) The factors causing the classification error were 'homospectral foreign bodies' and 'mixed pixels'. (3) When combined with the actual needs and image characteristics, the extensive use of medium and high-resolution remote sensing images to identify and monitor the surface elements of mining areas can greatly improve the work efficiency and minimize the image costs. (4) The construction layout of tailings pond in the Tebian coal mine was conducive

to reducing coal dust pollution. However, the long-term mixed use of tailings pond and spoil bank might cause accidents.(5) Coal dust pollution is concentrated in the surrounding areas of each mine pit.

Keywords: Wucaiwan mining area, unsupervised classification, supervised classification, object-oriented method, information extraction

Introduction

With the rapid development of economy, environmental problems such as air pollution [1-3], energy shortages [4] and water and soil loss [5-6] begin to appear. These problems are particularly serious in the mining area [7-9]. The local government needs to scientifically formulate pollution prevention and control policies according to the actual situation. Remote sensing technology can monitor the mining area in a large range for a long time, and can easily and quickly obtain the actual situation of the mining area. It is a common method of mining area management. Its advantages of low cost and high efficiency can make up for the high cost of manual investigation [10-11].

Many scholars at home and abroad use various methods to extract remote sensing image information to identify the distribution of ground features environmental pollution [12-15] Bhatti et al. [16]. proposed a local similarity projection Gabor filtering algorithm to classified hyperspectral images, and found that the classification accuracy of the method was much higher than others. Ahumada et al. [17]. used maximum likelihood methods to identify mining waste in the town of El Triunfo, Mexico, based on high-resolution multispectral images from the Pleiades satellite, and found that mining residues were present in 87.5% of the 32 zones. Dakuo et al. [18]. Proposed a tree root algorithm, combined with the limit learning method to build a classification model, and classified the multispectral image of Shenhua Baori Xile coal mine. It was found that compared with the traditional method, this method has the advantages of high precision, low cost and fast speed.

However, the above-mentioned research does not explain the applicability of each method to different scale remote sensing images of the same mining area. Accordingly, the classification effects of the different classification methods on the various research areas must be further discussed. This work takes the Landsat 8 image of the Wucaiwan mining area and the GF-2 image of the Tebian coal mine as the research object. Unsupervised classification, supervised classification and object-oriented classification are used to distinguish the surface elements of the mining area, compare various classification results and verify the accuracy. Moreover, the optimal classification method is used, the causes of classification errors are analysed, and the advantages of remote sensing monitoring combined with medium and high-resolution images are explained to

provide a method support for environmental monitoring and scientific management of the mining area.

Material and Methods

Study Area

The Wucaiwan mining area is located in Jimusar County, Xinjiang, China, as shown in Fig. 1. The area has a typical temperate continental arid climate. It is windy all year round, with wind force mostly levels 4-5 [19]. The average annual precipitation is approximately 100 mm. However, the annual evaporation can exceed 2000 mm, the sunshine period is long, and temperatures greatly vary during the day and night. The surface vegetation coverage is low, mainly gobi, bare land and rocks [20]. The mining area contains five large-scale open-pit coal mines, with a coal bearing area of approximately 900 km² and a proven coal resource reserve of 11.7 billion tons [21].

Data

The remote sensing data are downloaded from the official website of the geospatial data cloud (<http://www.gscloud.cn/>). Gaofen-2 (GF-2) satellite is the first civil optical remote sensing satellite independently developed by China with a spatial resolution better than 1m. It is equipped with two high-resolution 1 m panchromatic and 4 m multispectral cameras. It was successfully launched on August 19, 2014. Its high spatial resolution can realize high-precision monitoring of the ground [22]. Gf-2 image on September 11, 2018 is used in this paper. Landsat 8 satellite data is a remote sensing image with a spatial resolution of 30 m and a revisit period of 16 days. The satellite was successfully launched in the United States on February 11, 2013. It is equipped with a operational land imager and a thermal infrared sensor [23]. The image of Wucaiwan mining area on September 4, 2018 is used in this study.

The GF-2 image has a large amount of data. When a GF-2 image is used to classify the whole Wucaiwan mining area, the classification speed is slow. Accordingly, the Tebian coal mine with a relatively prominent pollution degree in the mining area and mature mining transportation storage and waste treatment system is selected as the research object of the GF-2 data. Landsat 8 image has smaller data volume, lower spatial resolution and faster classification speed compared with the GF-2 image. Therefore, the whole

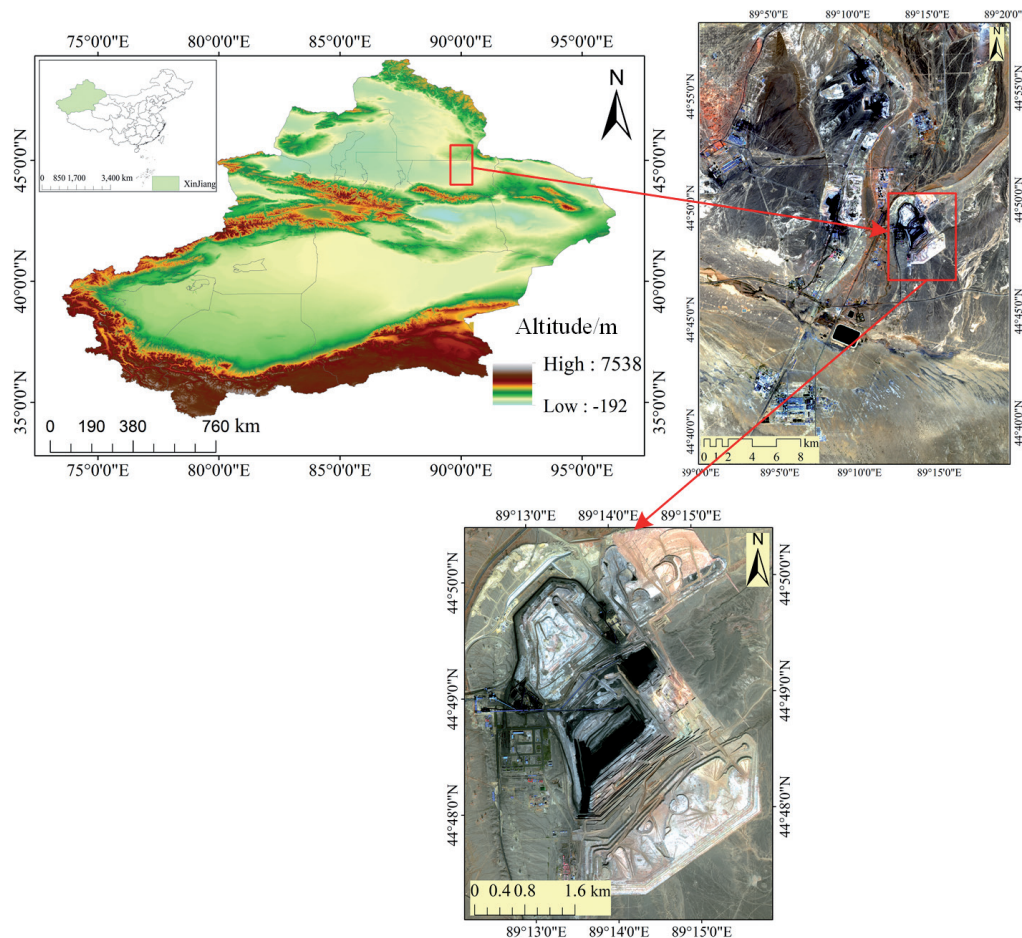


Fig. 1. Map of the study area.

Wucaiwai mining area is taken as the research object of Landsat 8 data.

Classification Methods

Unsupervised Classification

Unsupervised classification, also known as cluster analysis, refers to the classification of feature categories according to the statistical characteristics of the image itself and the distribution of natural point groups without prior knowledge of the study area [24-25].

ISOData method: The computer randomly selects some pixels as the initial clustering centre, and each clustering centre represents a class. Then, the computer calculates the distance between the pixel and the initial category centre, assigns the pixel to the nearest category to form the initial classification result and uses the clustering criteria to judge whether the initial classification result is reasonable. If the result is unreasonable, then the clustering centre is modified, and the aforementioned steps are continued; the iteration is carried out until the number of iterations is met [26-27]. The classification results obtained here are only spectral feature cluster groups. People also need to classify each

cluster group into a specific category according to the expert knowledge.

Supervised Classification

Supervised classification, also known as training site method, refers to the classification process of artificially selecting representative pixels as training samples of each category on the premise of extensive understanding of the study area; the computer is used to compare the differences between the pixels to be classified and the training samples, and each pixel is divided into a given category according to the classification rules of the selected classifier [28].

Mahalanobis distance method (MD): It is a method for evaluating the similarity between the pixel to be classified and the training sample. According to the Mahalanobis distance formula, the Mahalanobis distance is calculated from the pixel to be classified to the category with the shortest distance [29].

Support vector machine method(SVM): It is a machine learning method based on statistical learning theory, and it can automatically find the support vector with great discrimination ability for sample classification to construct a classifier for classification [30].

Maximum likelihood method (ML): Assuming that the training sample data follow the normal distribution in the spectral space, the eigenvalues of each training sample is first counted; then, the discriminant function is established, and the probability that the pixels to be classified belong to each category is calculated; the pixels are assigned to the category with the highest probability [31].

Minimum distance method (Min D): The mean and covariance matrix of each category are calculated according to the training sample data; the mean is taken as the central position of the category in the feature space, and the distance between the pixel to be classified and the centre of each category is calculated, pixels are divided into categories with the shortest distance [32].

Object-Oriented Classification

Object oriented classification (OOC) refers to merging pixels into several objects one by one according to the rule of minimum heterogeneity of pixel colour, shape and size. The spectral, texture and geometric features of each object contain many feature variables. The information of these feature variables is counted, and the classification rules of each category are defined by setting the parameters of feature variables to classify each object [33].

Object oriented classification includes nearest neighbour classification and membership classification. In this work, the nearest neighbour method is selected for object-oriented classification of remote sensing images.

Nearest neighbour method: Some objects are selected as the training samples of each category, the feature vector is taken as the centre, the Euclidean distance between the object to be classified and the training samples is calculated, and the object is divided into the category with the shortest distance [34].

Data Processing

The GF-2 and Landsat 8 images are preprocessed by Envi5.3 software, such as radiometric calibration, atmospheric correction, orthophoto correction, image fusion and image clipping. The two remote sensing images are visually interpreted. The interpretation results show that the GF-2 image contains tailings pond, coal dust, spoil bank, road, vegetation, water, buildings and gobi, for a total of eight types of surface elements.

Landsat 8 image contains seven types of surface elements: coal dust, buildings, water, mining areas, bare land, rocks, mining area and laterite.

In Envi5.3 software, the ISODATA classification parameters are set according to Table 1 to classify the GF-2 and Landsat 8 images in the study area. After the classification, the categories of the obtained cluster groups are merged and defined, and the images are outputted.

The GF-2 and Landsat 8 images are preprocessed by Envi5.3 software, such as radiometric calibration, atmospheric correction, orthophoto correction, image fusion and image clipping. The two remote sensing images are visually interpreted. The interpretation results show that the GF-2 image contains tailings pond, coal dust, spoil bank, road, vegetation, water, buildings and gobi, for a total of eight types of surface elements. Landsat 8 image contains seven types of surface elements: coal dust, buildings, water, mining areas, bare land, rocks, mining area and laterite.

In Envi5.3 software, the ISODATA classification parameters are set according to Table 1 to classify the GF-2 and Landsat 8 images in the study area. After the classification, the categories of the obtained cluster groups are merged and defined, and the images are outputted.

Results and Discussion

Analysis of the Classification Results

Analysis of the GF-2 Image Classification Results

The classification results of each method are shown in Figs 2 and 3. Figs 2 and 3 are compared and analysed in detail to understand the classification effects of the six methods on the GF-2 and Landsat 8 images:

ISOData: water and coal dust cannot be distinguished. The figure shows serious mixing between the spoil bank and the tailings pond. Except for the gobi, the classification boundary of other features is fuzzy, the feature information is broken, and the classification result is unreasonable.

MD: This method can clearly retain the texture information of the various surface elements and efficiently process their details. It can be seen that the coal dust pollution is mainly distributed in the downwind area of five mine pits. One deficiency is that this method wrongly divides a small amount of coal dust pixels around the pit into roads and some tailings pond pixels in the south of the pit into spoil banks. The overall classification results are consistent with the actual situation.

Min D: the information extraction of vegetation and buildings is relatively complete. However, this method wrongly divides some gobi pixels into roads, identifies a small amount of coal dust in the pit as water and mixes a large number of spoil bank pixels in the tailings pond

Table 1. Parameter setting of ISOData classification.

Image	Maximum number of iterations	Number of categories
GF-2	10	20
Landsat 8 OLI	15	15

in the south of the pit. The classification results are quite different from the actual situation.

ML: This method has some advantages in extracting large-area features. The outline of tailings pond, spoil bank and gobi in the figure is clear and complete. Nevertheless, this method wrongly divides a small number of gobi pixels near the pit into tailings pond, wrongly divides the gobi around the road into vegetation and identifies a small number of tailing pond pixels in the north of the pit as buildings, which is not suitable for the classification of small-area features.

SVM: the extraction results of roads, vegetation and buildings are accurate. However, this method misclassifies some gobi pixels in the east of the spoil bank into tailings pond and identifies a small number of tailings pond pixels as spoil bank. The extraction effect of coal dust and water is basically the same as that of the minimum distance method, and the overall classification result is reasonable.

OOC: The vegetation, water and road information in the mining area can be completely extracted. However, this method classifies many buildings and tailings pond, wrongly divides some gobi pixels into buildings and identifies certain gobi and spoil bank pixels as tailings pond. The overall classification effect is good.

Analysis of the Landsat 8 Image Classification Results

ISOData: Water, coal dust and rock are mixed together. There is only a general distinction between dark and light features. A large number of pixels in the mining area are identified as rocks, and part of the bare land is divided into sand and laterite. The classification results are quite different from the actual situation.

MD: the classification effect is good, the contour of the ground objects is clear, and the information is complete and intuitive. Only a small number of bare ground pixels are divided into rocks, and the overall classification result is consistent with the actual distribution of features.

Min D: The distribution of surface elements in the classification results is relatively concentrated. The identification ability of this method for coal dust is weak, and there is mixed classification amongst rock, bare land and mining area. Some pixels of bare land in the south of the mining area are wrongly divided into rock and mining area, and certain rock pixels around each pit are wrongly divided into bare land. A big gap is observed between the classification results and the actual situation.

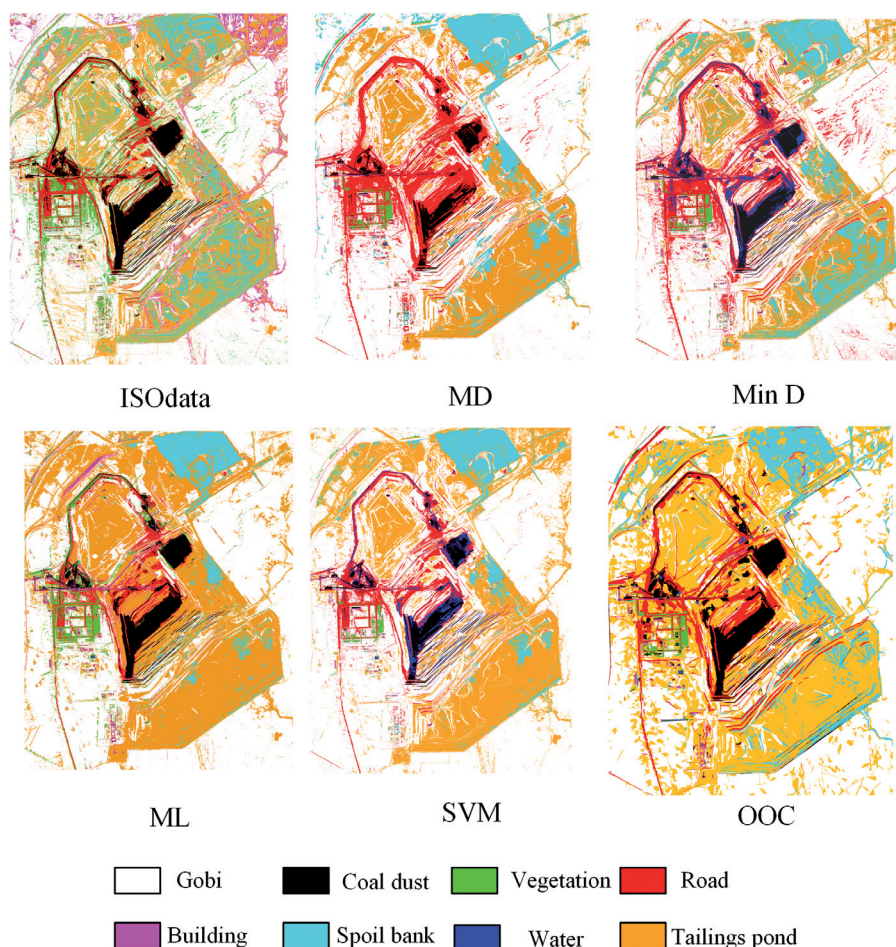


Fig. 2. GF-2 image classification results.

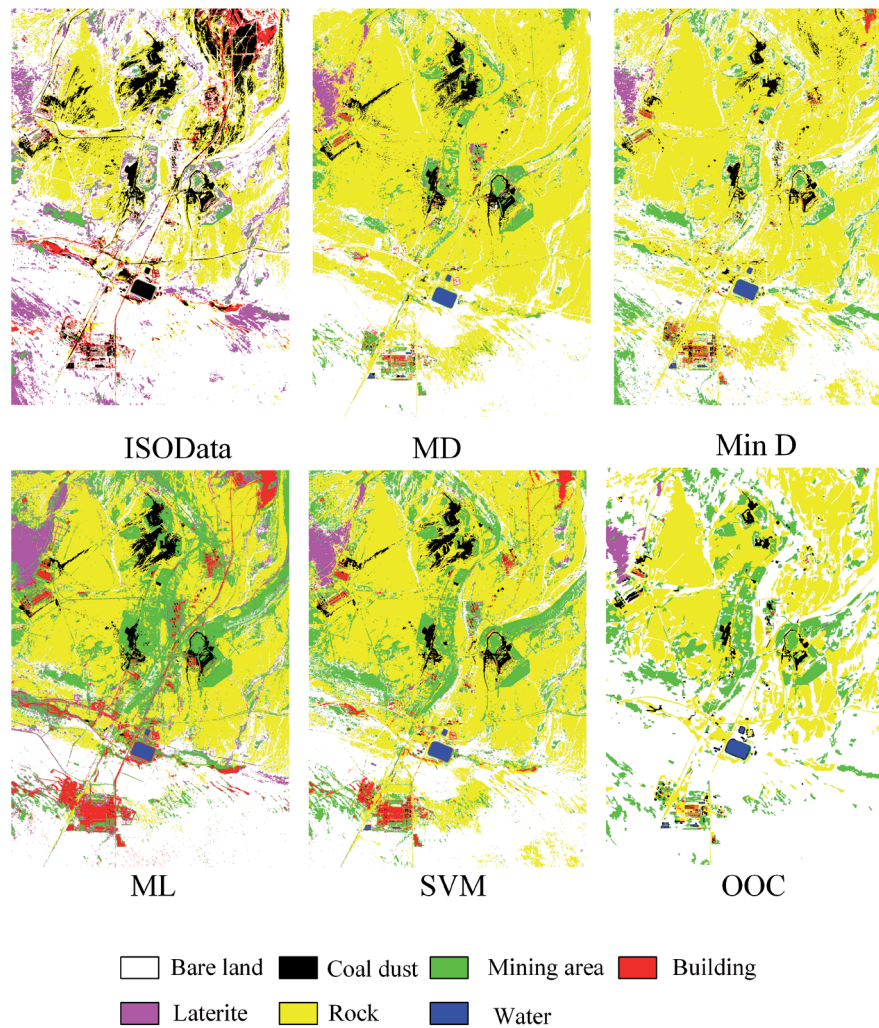


Fig. 3. Landsat 8 image classification results.

ML: The continuity between surface elements in the classification results is strong. However, this method identifies all white pixels in the mining area as mining areas and misclassifies some rocks in the northeast of the mining area into buildings. This method has a good extraction effect on large-area features, such as bare land and rocks, and poor recognition effect on small-area features, such as buildings, laterite and mining areas.

SVM: the classification results are similar to the maximum likelihood method, except that the continuity between the local table elements is weaker than the maximum likelihood method, and the rock pixels wrongly divided into mining areas and buildings are slightly less than the maximum likelihood method.

OOC: The coal dust pixels near the pit and on the road cannot be identified. The pixels are wrongly divided into rocks, many bare lands and mining areas are classified, and the rocks around the mining area are wrongly divided into bare lands. Meanwhile, the white rocks around the pit are wrongly divided into mining areas. The classification results are not ideal.

Accuracy Verification

Pixels or objects different from the training samples are selected as the verification samples to evaluate the classification effect of each method more objectively. The Kappa coefficient and overall classification accuracy of each classification result are obtained by calculating the confusion moment, as shown in Table 3. These factors are used as the basis for evaluating the classification effect. The larger the values of these indicators, the better the classification effect of this method.

Table 3 shows that when classifying GF-2 data, amongst the six methods, the Kappa coefficients of the Mahalanobis distance method, support vector machine method, maximum likelihood method and object-oriented method are more than 0.8, the overall classification accuracy is approximately 90%, and the classification effect is good. The Kappa coefficients of the ISODATA and minimum distance methods are below 0.8, and the overall classification accuracy is low.

The Mahalanobis distance method, maximum likelihood method and support vector machine method

Table 2. Parameter setting of object oriented classification.

Image	Segmentation scale	Shape factor	Compactness factor	Number of training samples	Feature vector
GF-2	100	0.8	0.5	376	Brightness, StD, Mean, Length/Width, Asymmetry, NDVI, NDWI
Landsat8	30	0.8	0.5	108	Mean

Table 3. Accuracy verification of image classification.

Classification method	GF-2		Landsat 8	
	Kappa coefficient	Overall accuracy /%	Kappa coefficient	Overall accuracy /%
ISOData	0.64	78.97	0.52	68.02
MD	0.90	94.27	0.85	90.02
OOC	0.85	89.68	0.66	75.52
ML	0.88	92.90	0.83	88.14
MinD	0.76	85.79	0.70	80.85
SVM	0.88	93.18	0.83	88.71

have higher classification accuracy amongst the six classification methods when extracting the feature information of Wucaiwan mining area based on Landsat 8 image. The Kappa coefficient is more than 0.8, the classification effect of Minimum distance method and object-oriented method is general, Kappa coefficient is between 0.6-0.8, and ISODATA method has the lowest classification accuracy, Kappa coefficient is lower than 0.6.

Analysis of the Optimal Classification Method

The overall classification accuracy of each method in Tables 3 and 4 is drawn into a bar chart to compare the applicability of each classification method to the GF-2 and Landsat 8 data, as shown in Fig. 4:

The aforementioned figure shows that a higher classification accuracy is obtain when the GF-2 image is used to monitor the surface elements of the mining area. However, the overall classification accuracy greatly varies when the ISODATA and object-oriented methods are used to classify the GF-2 and Landsat 8 data. When the Mahalanobis distance method, maximum

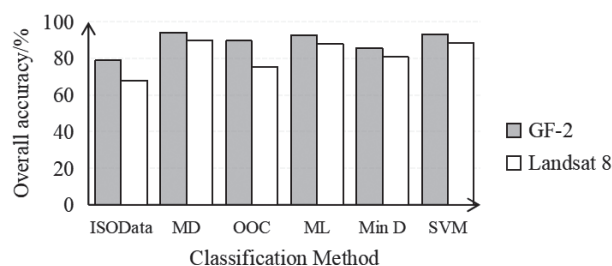


Fig. 4. Comparison of overall classification accuracy.

likelihood method, support vector machine method and minimum distance method are used to classify the two images, the overall classification accuracy slightly varies. This finding also shows that various methods have different applicability to medium and high-resolution image classification. The classification process and accuracy verification results are comprehensively compared. The applicability of each method to Landsat 8 image and GF-2 image classification is as follows:

Object-oriented approach: This method is more suitable for the classification of the GF-2 image compared with Landsat 8 image. However, the scale segmentation requires a substantial amount of time. After many experiments, the best combination of feature parameters is determined. Selecting many parameters may not improve the classification accuracy, but it will lead to dimension disaster, slow down the classification speed and choose few parameters; It will also reduce the accuracy of the classification results [35].

Mahalanobis distance method: This method is applicable to the classification of the GF-2 and Landsat 8 images. It has the advantages of simple steps, simple operation and fast running speed. It is not affected by the dimension and surrounding ground object pixels. It can take into account the internal changes of pixels. It is the optimal classification method and is more suitable for the actual spatial information extraction of mining.

Maximum likelihood method: The applicability to the GF-2 and Landsat 8 images in the study area is basically the same. However, this method can be easily affected by the surrounding ground features. The classification effect largely depends on the quantity and quality of training samples. When there are few training samples, the classification effect is poor.

Support vector machine method: From the perspective of classification process, support vector machine method is more suitable for Landsat 8 image classification because machine learning requires a large amount of time when using this method to classify GF-2 images. Moreover, only a small number of training samples can be selected before classification because the speed of machine learning will be greatly reduced with the increase in the number of training samples. This situation will result in a limited number of training samples for classifier learning, which may reduce the classification accuracy.

The ISODATA and minimum distance methods are not suitable for surface element recognition and monitoring of the GF-2 and Landsat 8 images in the study area.

Error Analysis

Different degrees of classification errors are observed in the classification results of each method in Fig. 3. The natural conditions, human activities and spectral characteristics of surface elements in the study area are analysed to explore the causes of this error. The result showed that the following two factors cause the classification error:

(1) The spectral reflectance curves of the various ground objects in the GF-2 and Landsat 8 images are drawn by using the spectral analytical tool in Envi5.3 software, as shown in Fig 5. In the GF-2 image, the change trend of spectral curve of spoil bank and tailings pond is roughly the same. In the Landsat 8 image, the change trend of spectral curve of rock, mining area and bare land is basically the same. The spectral characteristics of the white rock and mining area are similar. Accordingly, the above surface elements may be misclassified when using spectral features for classification due to the phenomenon of foreign matter in the same spectrum.

(2) Mixed pixel: Coal dust is easy to fly and diffuse. Over time, coal dust will accumulate on the road from the pit to the outside, forming a mixed pixel of

coal dust and road. Workers will spray water inside the pit to ensure construction safety; hence, there may be a mixture of water and coal dust in the pit. Industrial wastes may be stacked in the spoil bank and tailings pond, resulting in mixed pixels of tailings pond and spoil bank. Mixed pixels will affect the classification results because the specific category of mixed pixels is difficult to define.

Advantages of the Combination of GF-2 and Landsat 8 Data

In the actual operating process, remote sensing monitoring is easily affected by certain factors, such as terrain, funds, personnel and observation scale. Therefore, people need to select the appropriate remote sensing images and classification methods for mining area surface monitoring according to the project requirements.

The high spatial resolution of the GF-2 image can greatly improve the accuracy of remote sensing monitoring in the mining area. However, it is not practical to fully use the GF-2 data to monitor the mining area in a large area due to the limitations of classification speed and project funds. Therefore, the research and management of the mining area in combination with Landsat 8 medium-resolution and GF-2 high-resolution images can reduce the cost and solve the problem between monitoring accuracy and management cost to a certain extent.

During the large-scale classification and monitoring of the mining areas using Landsat 8 images, supplementing Landsat 8 images with GF-2 data can save cost and improve classification quality when some surface elements are difficult to identify due to spatial resolution.

Distribution of Surface Elements

Landsat 8 images show that rocks and bare land are widely distributed in the whole Wucaiwan mining area, and coal dust is concentrated near the main pit, factory

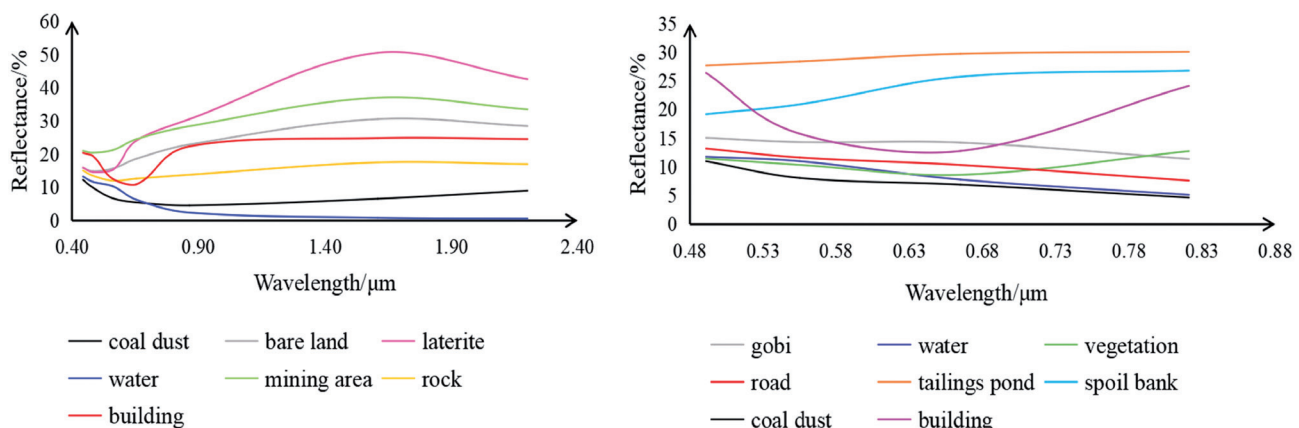


Fig. 5. Spectral curves of ground objects.

buildings and roads. Further observation is made on the Tebian coal mine with the help of the GF-2 image to explore the reason why coal dust is concentrated in local areas. The result showed that the tailings pond in the Tebian coal mine is built in the southeast of the pit and is in the downwind direction of the pit (the dominant wind direction is northwest wind), which can block the diffusion path of coal dust to a certain extent. Thus, it plays a positive role in reducing the scope of coal dust pollution in the mining area.

The GF-2 image depicts that the mixing of tailings pond and spoil bank in the Tebian coal mine is serious. The field investigation result shows that local factories stack industrial wastes that should have been discharged in the spoil bank in the tailings pond. If things go on like this, then the dam body of the tailings pond will be unstable and cause landslide once the accumulated industrial wastes and tailings exceed the bearing range of the tailings pond. However, industrial wastes can form relatively solid rock shells on the dam surface, which can effectively prevent the secondary pollution of surface dust.

Conclusions

This work identifies the surface elements in the Landsat 8 image of the Wucaiwan mining area and GF-2 image of the Tebian coal mine through unsupervised classification, supervised classification and object-oriented classification. Moreover, this work compares the classification results of each method and verifies the accuracy. The following conclusions are formulated:

(1) The comparison result of the operating process and classification accuracy shows that the Mahalanobis distance method has the best classification effect. This method has high classification accuracy for the GF-2 and Landsat 8 images. When classifying GF-2 images, the Kappa coefficient reaches 0.90, and the overall classification accuracy is 94.27%. When classifying Landsat 8 images, the Kappa coefficient reaches 0.82, and the overall classification accuracy is 87.23.

(2) The factors causing the classification error are 'homospectral foreign bodies' and 'mixed pixels'.

(3) In combination with the actual needs and image characteristics, the comprehensive use of medium and high-resolution remote sensing images to identify and monitor the surface elements of mining areas can greatly improve the work efficiency and reduce the image cost.

(4) Coal dust pollution is concentrated in the surrounding areas of each mine pit. The construction layout of tailings pond is conducive to reducing coal dust pollution. However, the long-term mixed use of tailings pond and spoil bank may cause accidents.

Acknowledgments

This research was funded by the Xinjiang Uygur Autonomous Region University Scientific Research Program Project (No.XJEDU2021Y011).

Conflict of Interest

The authors declare no conflict of interest.

References

- SUN Y.P., LI Y.Y., YU T.T., ZHANG X.Y., LIU L.N., ZHANG, P. Resource extraction, environmental pollution and economic development: Evidence from prefecture-level cities in China. *Resources Policy*, **74**, 102330, **2021**.
- BHATTI U.A., ZEESHAN Z., NIZAMANI M.M., BAZAI S., YU Z., YUAN L. Assessing the change of ambient air quality patterns in Jiangsu Province of China pre-to post-COVID-19. *Chemosphere*, **288** (2), 132569, **2022**.
- ZHANG G.X., JIA Y.Q., SU B., XIU J. Environmental regulation, economic development and air pollution in the cities of China: Spatial econometric analysis based on policy scoring and satellite data. *Journal of Cleaner Production*, **328**, 129496, **2021**.
- XU Z.C., CHAU S.N., CHEN X.Z., ZHANG J., LI Y.J., DIETZ T., WANG J.Y., WINKLER J.A., FAN F., HUANG, B.R. Assessing progress towards sustainable development over space and time. *Nature*, **592** (7856), E28, **2021**.
- CHEN T., SHU J., HAN L., TIAN G., YANG G., LV J. Modeling the effects of topography and slope gradient of an artificially formed slope on runoff, sediment yield, water and soil loss of sandy soil. *Catena*, **212**, 106060, **2022**.
- ANTONELI V., DE PAULA E.C., BEDNARZ J.A., RODRIGO-COMINO J., CERDA A., PULIDO M. Soil and water losses along the cultivation cycle of onion in Irati, Brazil. *Catena*, **204**, 105439, **2021**.
- LI Y., CHI Y.H., LIN T.Y. Coal production efficiency and land destruction in China's coal mining industry. *Resources Policy*, **63**, 101449, **2019**.
- KHARISOVA O., KHARISOV T. Searching for possible precursors of mining-induced ground collapse using long-term geodetic monitoring data. *Engineering Geology*, **289**, 106173, **2021**.
- RUDKE A.P., SIKORA DE SOUZA V.A., DOS SANTOS A.M., FREITAS XAVIER A.C., ROTUNNO FILHO O.C. MARTINS J.A. Impact of mining activities on areas of environmental protection in the southwest of the Amazon: A GIS- and remote sensing-based assessment. *Journal of Environmental Management*, **263**, 110392, **2020**.
- FIROZJAEI M.K., SEDIGHI A., FIROZJAEI H.K., KIAVARZ M., PANAH S. A historical and future impact assessment of mining activities on surface biophysical characteristics change: A remote sensing-based approach. *Ecological Indicators*, **122**, 107264, **2021**.
- LI H., XU F., LI Q. Remote sensing monitoring of land damage and restoration in rare earth mining areas in 6 counties in southern Jiangxi based on multisource sequential images. *Journal of Environmental Management*, **267**, 110653, **2020**.

12. BHATTI U.A., MING-QUAN Z., QING-SONG H., ALI S., HUSSAIN, A., YUHUAN Y., YU Z., YUAN L., NAWAZ S.A. Advanced Color Edge Detection Using Clifford Algebra in Satellite Images. *IEEE Photonics Journal*, **13** (2), 1, **2021**.
13. YU H.Y., CHENG G., GE X.S., LU X.P. Object oriented land cover classification using ALS and GeoEye imagery over mining area. *Transactions of nonferrous metals society of China*, **21**, 733, **2011**.
14. DONG B.S., YANG Y., CUI Q. Detailed Classification and Analysis Based on Separator No. 2 Land Use in Mining Area. *Journal of Gansu Science*. **31** (01), 81, **2019** [In Chinese].
15. HUANGFU R., LI A. Contrastive Analysis of Extraction Methods for Ground Object Information in Mining Area Based on Remote Sensing Image. *Journal of Tangshan University*. **33** (03), 42, **2020** [In Chinese].
16. BHATTI U. A., YU Z., CHANUSSOT J., ZEESHAN Z., YUAN L., LUO W., NAWAZ S.A., BHATTI M.A., UL AIN Q., MEHMOOD A. Local Similarity-Based Spatial-Spectral Fusion Hyperspectral Image Classification With Deep CNN and Gabor Filtering. *IEEE Transactions on Geoscience and Remote Sensing*. **60**, 1, **2021**.
17. AHUMADA-MEXÍA R., MURILLO-JIMÉNEZ J.M., ORTEGA-RUBIO A., MARMOLEJO-RODRÍGUEZ A.J., NAVA-SÁNCHEZ E.H. Identification of mining waste using remote sensing technique: A case study in El Triunfo town, BCS, México. *Remote Sensing Applications: Society and Environment*, **22**, 100493, **2021**.
18. HE D.K., LE B.T., XIAO D., MAO Y.C., SHAN F., HA T.T.L. Coal mine area monitoring method by machine learning and multispectral remote sensing images. *Infrared Physics & Technology*, **103**, 103070, **2019**.
19. SAWUT R., TIYIP T., ABLIZ A., KASIM N., NURMEMET I., SAWUT M., TASHPOLAT N., ABLIMIT A. Using regression model to identify and evaluate heavy metal pollution sources in an open pit coal mine area, Eastern Junggar, China. *Environmental Earth Sciences*, **76** (24), 822, **2017**.
20. MA X.T., YIN J.Q., CHENG Y., WANG X.Y. Research on open-pit coal mine environmental performance evaluation based on PSR model in desert region. *China Coal*. **41** (03), 126, **2015** [In Chinese].
21. XIA N., TIYIP T., ZHANG F. Spatio-temporal variation of land surface temperature in the coalmine area of Zhundong in Xinjiang. *China Mining Magazine*. **25** (1), 69, **2016**.
22. SHEN G., XU B., JIN Y.X., CHEN S., ZHANG W.B., GUO J., LIU H., ZHANG Y.J., YANG X.C. Monitoring wind farms occupying grasslands based on remote-sensing data from China's GF-2 HD satellite – A case study of Jiuquan city, Gansu province, China. *Resources Conservation & Recycling*. **121**, 128, **2016**.
23. LI P., CHEN S.L., JI H.Y., KE Y., FU Y.T. Combining Landsat-8 and Sentinel-2 to investigate seasonal changes of suspended particulate matter off the abandoned distributary mouths of Yellow River Delta. *Marine Geology*, **441**, 106622, **2021**.
24. LIU J.G., MASON P.J. *Essential Image Processing and GIS for Remote Sensing*. John Wiley & Sons, **2013**.
25. OZESMI S.L., BAUER M.E. Satellite remote sensing of wetlands. *Wetlands Ecology and Management*, **10** (5), 381, **2002**.
26. BALL G.H., HALL D.J. ISODATA, a novel method of data analysis and pattern classification. *Stanford research inst. CA: Menlo Park*. **1965**.
27. VENKATESWARLU N., RAJU P. Fast ISODATA clustering algorithms. *Pattern Recognition*. **25**, 335, **1992**.
28. YANG X. An Elementary Introduction to Supervised and Unsupervised Classification of Remote Sensing Image. *Acta Geologica Sichuan*, **03**, 251, **2008**.
29. SUN G.Y., RONG X.Q., ZHANG A.Z., HUANG H., RONG J., ZHANG X.M. Multi-Scale Mahalanobis Kernel-Based Support Vector Machine for Classification of High-Resolution Remote Sensing Images. *Cognitive Computation*, **13** (4), 787, **2021**.
30. GARCIA M., RIANO D., CHUVIECO E., SALAS J., DANSON F. M. Multispectral and LiDAR data fusion for fuel type mapping using Support Vector Machine and decision rules. *Remote Sensing of Environment*, **115** (6), 1369, **2011**.
31. LIU K.F., SHI W.Z., ZHANG H. A fuzzy topology-based maximum likelihood classification. *ISPRS Journal of Photogrammetry and Remote Sensing*, **66** (1), 103, **2011**.
32. FAN H.Y., DONG W., KANG B.S., ZHANG D.Q. Remote sensing image-based comparison of methods for mountain glacier identification. *Water Resources and Hydropower Engineering*, **51** (5), 47, **2020** [In Chinese].
33. WEN Y.T., ZHAO J., LAN Y.B., YANG D.J., PAN F.J., CAO D.L. Classifications of Tree Species Based on UAV's Visible Light Images and Object-Oriented Method. *Journal of Northwest Forestry University*, **37** (01), 74, **2022** [In Chinese].
34. JIA M. Information extraction and dynamic monitoring of open-pit mining area based on remote sensing technology. *North China University of Technology, M. Sc. Thesis*. **2020** [In Chinese].
35. WANG Y.J., MENG Q.Y., YANG J., SUN Y.X., LI P., XING W.J. Object Based Remote Sensing Image Classification Based on Feature Selection Method. *Science, Technology and Engineering*, **16** (32), 107, **2016** [In Chinese].